Dear Author,

Please, note that changes made to the HTML content will be added to the article before publication, but are not reflected in this PDF.

Note also that this file should not be used for submitting corrections.

Surface Science xxx (2015) xxx–xxx

Contents lists available at ScienceDirect

Surface Science

journal homepage: www.elsevier.com/locate/susc

Synthesis of nitrogen-doped epitaxial graphene via plasma-assisted method: Role of the graphene–substrate interaction

Fabrizio Orlando [a,1], Paolo Lacovig [b], Matteo Dalmiglio [b], Alessandro Baraldi [a,b,c], Rosanna Larciprete [d], Silvano Lizzit [b,*]

[a] Physics Department, University of Trieste, Via Valerio 2, 34127 Trieste, Italy
[b] Elettra-Sincrotrone Trieste S.C.p.A., AREA Science Park, S.S. 14 km 163.5, 34149 Trieste, Italy
[c] IOM-CNR, Laboratorio TASC, AREA Science Park, S.S. 14 km 163.5, 34149, Trieste, Italy
[d] CNR-Institute for Complex Systems, Via Fosso del Cavaliere 100, 00133 Roma, Italy

ARTICLE INFO

Available online xxxx

Keywords:
Graphene
Functionalization
Nitrogen doping
XPS
XPD
Iridium

ABSTRACT

Functionalization of graphene by substitution of the carbon with nitrogen atoms is a promising way to tailor its electronic properties, but a good control over the heteroatomic configuration in the graphene network is most often a difficult task. In this paper, the synthesis of N-doped graphene by nitrogen plasma treatment of graphene/Ir(111) is presented. The formation of substitutional, pyrrolic and pyridinic nitrogen is analyzed by means of X-ray photoelectron spectroscopy (XPS) and X-ray photoelectron diffraction (XPD). The graphene–Ir interaction is suggested to control the variation in the relative concentration of the nitrogen species. Annealing of the sample also leads to modifications of the nitrogen species incorporated in the graphene layer. Furthermore, the connection of the substitutional nitrogen arrangement with its corresponding spectroscopic fingerprint is unequivocally confirmed by XPD measurements which give also a direct insight on the local geometry of the nitrogen atoms incorporated in the carbon network.

1. Introduction

The combination of many outstanding properties in a single material makes graphene (GR) really attractive for a number of technological applications. In this regard, the use of graphene single layers into high-performance integrated circuits is one of the most intriguing prospects. However, the absence of a gap in its band structure, sets severe limits on the use of graphene in, e.g., transistors because of the low on–off ratio achievable [1]. This is the reason why the opening and fine tuning of an energy gap in the band structure of graphene has been an issue of fundamental importance since its discovery. Different routes have been followed to tailor the electronic properties of graphene. The first to be explored were methods based on the morphology control over the graphene structure. For instance, by making graphene nanoribbons it is possible to laterally confine the charge carriers. In nanoribbons, different types of edges show either metallic (zigzag edge) or semiconducting (armchair edge) character [2]. Furthermore, the possibility of opening a band gap in bilayer graphene by applying a strong electric field [3] or by selectively controlling the carrier density in each layer [4] was also explored. However, these approaches resulted in a small band gap or in a strong degradation of the carrier mobility [1].

A promising alternative approach to modify the electronic properties of graphene is by chemical doping, which can be achieved by patterning the graphene surface with atoms [5] or molecules [6], or by introducing heteroatoms in the carbon network [7]. In the latter case, the substitution of carbon with nitrogen or boron atoms is of considerable interest not only because the shift of the energy of the Dirac point leading to n- or p-doped graphene could be achieved, but also because the characteristic features of the graphene electronic band structure could be modified [8]. For sp^2 carbon structures, like graphene or carbon nanotubes, the incorporation of nitrogen in the lattice has been already demonstrated to be a robust and efficient method to tune the electronic properties with only minor structural perturbations, due to the possibility to form covalent bonds [9,10].

Several methods have been developed to synthesize N-doped graphene. For instance, direct synthesis of N-doped graphene can be achieved by chemical vapor deposition (CVD) [11] or arc discharge [12] approaches. On the other hand, post-synthesis methods are also widely used, such as thermal annealing [13] in ammonia (NH_3) atmosphere or plasma treatment [14,15]. Although different atomic arrangements of the nitrogen atoms in the carbon network are possible (some of them are displayed in the top panel of Fig. 1), three main configurations have been characterized namely graphitic, also known as substitutional, pyridinic and pyrrolic nitrogen. Several characterization tools

* Corresponding author.
E-mail address: silvano.lizzit@elettra.eu (S. Lizzit).
[1] Present address: Laboratory of Radiochemistry and Environmental Chemistry, Paul Scherrer Institut, 5232 Villigen, Switzerland.

http://dx.doi.org/10.1016/j.susc.2015.06.017
0039-6028/

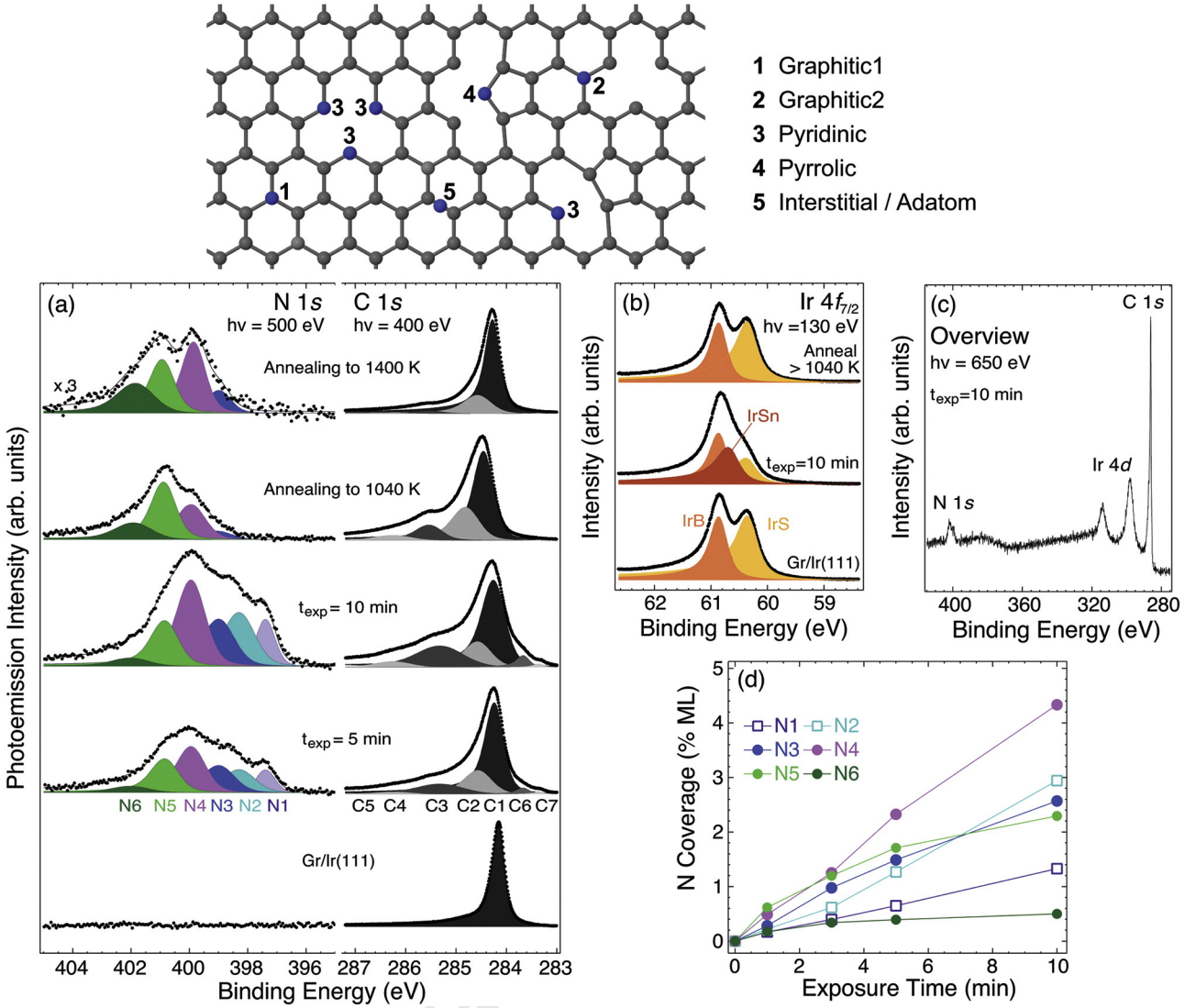

Fig. 1. (color online) (a) Evolution of N 1s and C 1s core levels after subsequent exposures of GR/Ir(111) to N plasma and after annealing to 1040 K and 1400 K. The filled peaks represent the spectral components as resulting from the deconvolution procedure (see main text for more details). (b) Comparison between the Ir $4f_{7/2}$ core level measured for the pristine GR/Ir(111) (bottom), after 10 min of exposure to N plasma (middle) and after annealing to 1040 K (top). (c) Overview spectrum measured after 10 min of exposure to N plasma. (d) Coverage of the distinct N species during exposure of GR/Ir(111) to N plasma, as determined from the fitting of the spectra in (a). The top picture shows a schematic representation of the nitrogen configurations discussed in the paper: 1 and 2 are graphitic-N atoms within an intact graphene region and neighboring a defect site, respectively; 3 and 4 are N atoms in pyridinic and pyrrolic configuration while 5 is N atoms adsorbed on the graphene basal plane or in interstitial position.

based on microscopy and spectroscopy have been used to investigate the N-doped graphene layers (e.g. scanning tunneling microscopy (STM) [16,17], transmission electron microscopy (TEM) [18], X-ray photoelectron spectroscopy (XPS) [9,10] and Raman spectroscopy [11,19]), but the connection between the nitrogen bonding configuration and the synthesis method is not always straightforward.

Motivated by this lack of information, we exploited the potential offered by XPS and X-ray photoelectron diffraction (XPD) techniques to study the functionalization and to determine the surface structure of a N-doped graphene layer produced upon nitrogen plasma exposure of the GR/Ir(111) interface. In this paper we illustrate how a combined XPS and XPD investigation can provide insight into the correlation between the electronic and structural properties of N-doped graphene.

2. Material and methods

The experiments were performed at the SuperESCA beamline of Elettra, the synchrotron radiation facility in Trieste, Italy. The Ir(111) single crystal was cleaned by repeated cycles of Ar^+ sputtering and annealing in O_2 atmosphere between 600 and 1100 K, followed by hydrogen exposure at 800 K to remove the residual oxygen. The graphene monolayer was grown on Ir(111) by doing 10 cycles of temperature-programmed growth, consisting in dosing ethylene at 520 K and annealing to 1470 K, followed by a prolonged annealing at high temperature with a base ethylene pressure of 1×10^{-7} mbar. This procedure ensures the growth of a complete layer of graphene that does not leave bare Ir regions. The as-grown graphene layer was then exposed to nitrogen plasma at room temperature using a Gen2 plasma source from Tectra GmbH, configured as atom source without ion-trap. Within this mode of operation the beam is mainly composed by neutral atoms with a fraction of residual ions with energy of about 25 eV, defined by the intrinsic plasma potential. Different conditions such as N_2 pressure, position of the sample surface with respect to the source and exposure time were tested. An efficient nitruration of graphene was achieved for exposures with N_2 base pressure of 2.5×10^{-5} mbar performed with the Ir surface placed in front of the plasma source.

The high-energy resolution XPS spectra of the Ir $4f_{7/2}$, C 1s and N 1s core levels were measured in normal emission (in the present setup this corresponds to 70° of incidence of the photon beam) using photon

Please cite this article as: F. Orlando, et al., Synthesis of nitrogen-doped epitaxial graphene via plasma-assisted method: Role of the graphene–substrate interaction, Surf. Sci. (2015), http://dx.doi.org/10.1016/j.susc.2015.06.017

energies of 130, 400 and 500 eV, respectively, with an overall energy resolution ranging from 40 to 100 meV. The core level binding energy scale was referred to the Fermi level of the Ir substrate measured in the same conditions. The spectra were fitted with Doniach-Šunjić functions [20] convoluted with a Gaussian, and a linear background. The nitrogen concentration was determined from survey spectra measured at 650 eV by calculating the ratio of the N 1s and C 1s intensities properly normalized for the respective photoemission cross section at this photon energy.

The XPD measurements of the N1s core level were performed with photon energy of 500 eV corresponding to an electron kinetic energy of 100 eV. The diffraction patterns were measured over an azimuthal sector of 120°, from normal ($\theta = 0°$) to grazing emission ($\theta = 80°$). The modulation functions were obtained for each polar emission angle θ from the peak intensity $I(\theta,\Phi)$ as $(I(\theta,\Phi) - I_0(\theta)) / I_0(\theta)$, where $I_0(\theta)$ is the average value of each azimuthal scan. The simulations were performed with the Electron Diffraction in Atomic Cluster (EDAC) package [21] for a free-standing, flat graphene layer with a N atom in graphitic configuration as emitter. The inclusion of the Ir substrate in the simulations, does not produce appreciable differences in the XPD patterns, because of the lattice mismatch between graphene and Ir(111). Indeed, any N atom in graphitic configuration within a moiré unit cell does not have a specific local geometry with respect to the Ir atoms thus smearing out the diffraction from the Ir substrate.

3. Results and discussion

As a first step, we followed the evolution of the N 1s, C 1s and Ir $4f_{7/2}$ core level spectra as a function of the nitrogen plasma exposure on GR/Ir(111). We performed 5 cycles for a total dosing time of 10 min, as shown in Fig. 1. The final nitrogen concentration was estimated to be 0.14 ML with respect to graphene, as determined from the overview spectrum of Fig. 1c. From the beginning of nitrogen exposure (Fig. 1a), the N 1s core level region exhibits a broad spectrum, where six different components have to be set in order to fit the uptake series. These components arise from nitrogen atoms in different chemical environments: N1 (397.4 eV), N2 (398.3 eV), N3 (399.0 eV), N4 (400.0 eV), N5 (400.9 eV) and N6 (401.9 eV). Fig. 1d shows the evolution of the N 1s components as a function of dosing time. It appears quite clear that N5 and N6 display the same behavior approaching almost saturation after a dosing time of 10 min, while the other components keep on increasing almost linearly. The N2–N6 components fall in the binding energy range of the graphitic (N5, N6), pyrrolic (N4) and pyridinic (N2, N3) nitrogen, as previously reported [9,11,13,15,19,22–26], but their assignment to specific nitrogen species is not straightforward. Indeed, other configurations may be possible, including nitrogen adatoms or interstitial nitrogen as most of the nitrogen plasma impinging on the surface is composed by N atoms that could adsorb on GR. The Ir substrate may also play an important role in GR functionalization [5,27], even if GR/Ir(111) is a weakly interacting system [28,29]. Based on the XPD investigation described below and according to Refs. [15] and [30], we attribute N5 and N6 to graphitic-like N atoms, placed within an intact graphene region and neighboring a defect site, respectively (denoted as graphitic1 and graphitic2 in the top part of Fig. 1). The position of N1 is in the range of the binding energies measured for nitrogen atoms adsorbed on the Ir(111) surface dosed with NH_3 [31]. Also in the present study we observed a single N 1s peak centered at 397.4 eV after nitrogen plasma dose on the clean Ir(111) surface (top curve of Fig. 2c). Therefore, we assign N1 to nitrogen atoms that intercalate below graphene and chemisorb on the Ir substrate. As illustrated in Fig. 1a, the relatively high intensity of N1 indicates that a sizeable amount of N atoms intercalate underneath the graphene layer. The intercalation process may take place at pre-existing graphene defects or wrinkles, as already suggested for O_2 intercalation on GR/Ir(111) [32]. However, in the present case it is more likely that the nitrogen ions from the plasma source introduce defects in graphene: the carbon network is damaged upon nitrogen plasma exposure, thus fostering further intercalation.

The growth of the different components in the N 1s core level region is paralleled by a broadening of the C 1s spectrum (Fig. 1a) reflecting the changes of the graphene lattice induced by the nitrogen plasma treatment which eventually causes also the incorporation of nitrogen atoms in the graphene network. As a result, the main C 1s peak (C1) related to sp^2 bonded C–C atoms broadens and shifts towards higher binding energy with respect to the value measured for the clean graphene (284.14 eV), and several other components appear at higher and lower binding energy: C2 (284.54 eV), C3 (285.26 eV), C4 (286.20 eV), C5 (287.10 eV), C6 (283.65 eV) and C7 (283.35 eV). It has to be noted that the total intensity in the C 1s region keeps constant during nitruration. While C6 and C7 could be attributed to carbon vacancies [33] and to C atoms at the Ir steps [28], respectively, the interpretation of the C2–C5 components is not straightforward. Indeed, their large width indicates that they can include contributions from different configurations of the carbon atoms. We tentatively assign C3–C5 peaks to sp^2 and sp^3 C–N bonds [34] while C2 may be attributed to the carbon atoms second-nearest neighbors to a graphitic-N, similarly to the case of a planar 3-fold C–O configuration resulting from the inclusion of an oxygen atom in a carbon vacancy [33]. However, calculations similar to those performed in Ref. [33] would be required in order to clarify this issue.

The variations in the chemical composition of the graphene layer lead to noticeable changes also in the Ir $4f_{7/2}$ spectra (Fig. 1b). The Ir $4f_{7/2}$ spectrum of pristine GR/Ir(111) consists of two components, representing bulk (IrB at 60.84 eV) and surface (IrS at 60.31 eV) atoms, and it is comparable to that of clean Ir(111) [35] because of the low interaction between the graphene layer and the substrate [28]. Upon nitrogen plasma treatment, a new component IrSn appears between the surface and the bulk peaks at 60.70 eV, which grows at the expense of the surface component IrS, due to the adsorption of the intercalated nitrogen and to the interaction of the N-doped graphene with the iridium substrate.

With the aim of determining the role of the Ir substrate in nitrogen functionalization of GR/Ir(111), we performed identical nitrogen plasma treatments on a quasi free-standing graphene layer obtained by intercalating oxygen under graphene [32]. Fig. 2 shows the N 1s core levels of the GR/O/Ir(111) system during nitrogen plasma treatment. The comparison between the spectra measured after 10 min plasma exposure on GR/Ir(111) and GR/O/Ir(111) shows that the overall N coverage decreases to 0.1 ML in the latter case. On the other hand big differences in the relative concentration of the nitrogen species are quite evident from the comparison of Fig. 2b with Fig. 1d. More precisely, the N1 intensity, i.e. the amount of nitrogen adsorbed on the Ir substrate, is practically unchanged, N5 and N6 increase, N2 slightly decreases while N3 and N4 drop to half of their respective intensity for the Gr/Ir(111) system. As a result, the absolute coverage of graphitic-N species (N5 + N6) goes from 0.028 ML to 0.036 ML and their concentration with respect to the other nitrogen species bound to graphene (N2 + N3 + N4) increases from 28% to 60%.

The comparison between the two experiments described above clearly highlights the influence of the substrate on the functionalization of the graphene layer. The GR–Ir interaction, albeit weak, fosters the formation of the pyridinic and pyrrolic nitrogen species. In addition, the formation of graphitic-N can be hindered in the valleys of the moiré corrugation of GR/Ir(111) [28], where the bonding between C and Ir atoms is stronger. It is worth noting that a number of studies have previously demonstrated the crucial role of the weak interaction of graphene with the underlying Ir(111) substrate and, in particular, of the template structure of this interface. For instance, the coupling to the substrate controls the patterned adsorption of hydrogen on GR/Ir(111) [5,27], drives the (de)oxidation processes during thermal reduction of graphene oxide [36], allows to fine tune the morphology of nanoclusters [37,38] an can even affect charge transfer processes of photo-excited

Please cite this article as: F. Orlando, et al., Synthesis of nitrogen-doped epitaxial graphene via plasma-assisted method: Role of the graphene–substrate interaction, Surf. Sci. (2015), http://dx.doi.org/10.1016/j.susc.2015.06.017

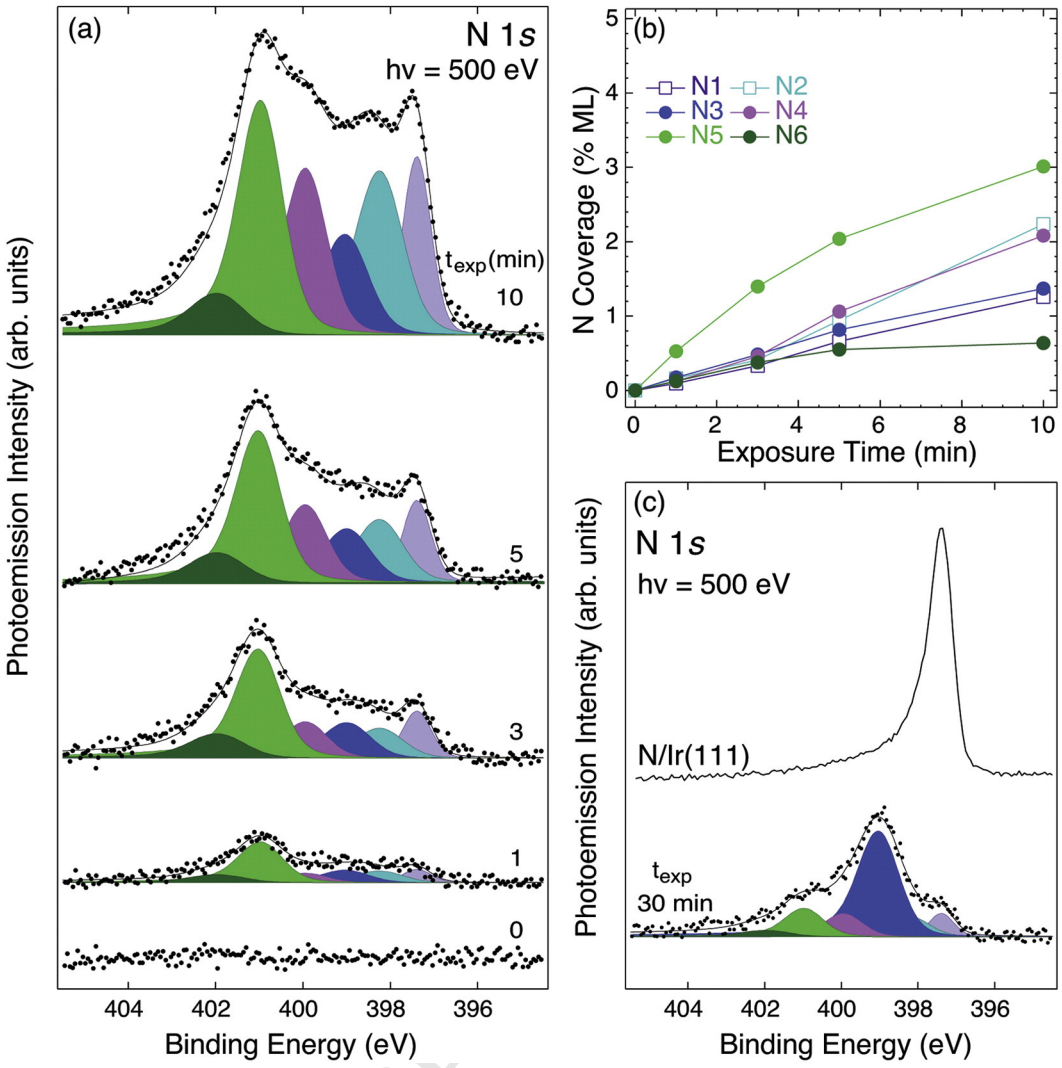

Fig. 2. (color online) (a) Evolution of the N 1s core level after subsequent exposures of GR/O/Ir(111) to nitrogen plasma. The filled peaks represent the spectral components as resulting from the deconvolution procedure. (b) Coverage of the distinct N species during exposure of GR/O/Ir(111) to N plasma as determined from the fitting of the spectra in (a). (c) Bottom: N 1s spectrum measured after 30 min of exposure of GR/Ir(111) to N plasma, with the sample placed outside the emission cone of the plasma source in order to avoid N ions dosing. Top: N 1s spectrum measured after saturation of the bare Ir(111) surface with atomic N from the plasma source.

electrons [39]. On the other hand, the suppression of the GR–Ir interaction upon oxygen intercalation leads to significant reduction of the pyridinic and pyrrolic-N content, suggesting that these configurations are stabilized by the presence of the Ir surface.

In order to highlight the contribution of the N atoms we dosed for 30 min the sample rotated with respect to the emission cone of the source in order to avoid hitting the surface with nitrogen ions. The bottom spectrum in Fig. 2c shows the resulting N1s spectrum. As the carbon network should be less damaged by this treatment with respect to the standard exposure geometry (Figs. 1 and 2), it is reasonable to assume that most of the nitrogen atoms are now adsorbed on graphene or in interstitial positions and do not form pyridinic species which need the formation of a defect. Indeed, the resulting N1s spectrum is composed mainly by one peak, which coincides with N3. This gives a strong indication that the adatoms contribute to the N3 component. Moreover, this finding suggests that in order to form graphitic, pyridinic and pyrrolic species, energetic nitrogen ions are required to break the C–C bonds. The chemical doping of graphene is therefore achieved only if defects are introduced in the carbon network by kinetic impact with the energetic ions.

In order to shed light on the thermal stability of the N-doped graphene we performed a thermal desorption experiment while monitoring the N 1s core level region. The central panel in Fig. 3a shows the intensity plot derived from the Temperature Programmed XPS (TP-XPS) [40] N 1s spectra acquired while annealing the sample up to 1040 K. The N 1s spectra measured at room temperature before and after the annealing are reported at the bottom and top of Fig. 3a, respectively, while the quantitative analysis of the TP-XPS spectra is displayed in Fig. 3b. In Fig. 1a the corresponding C 1s spectra are shown. Upon annealing, the total amount of nitrogen goes from 0.14 ML to 0.06 ML, the relative concentration of the nitrogen species changes and the C 1s peak narrows losing about 5% of its initial intensity. The most interesting aspect of the annealing process is the conversion of part of the nitrogen species into graphitic-N between 400 and 900 K, as indicated by the significant increase of N5 and N6 at the expense of all other components in this temperature range. It should be noted that the rearrangement of nitrogen species upon annealing has been already observed for similar interfaces [9,23,41]. The behavior of the atomic nitrogen component N1, which disappears above 800 K, resembles that observed on the pristine Ir(111) surface, where the nitrogen atoms desorb as N_2 between 400 and 700 K [31]. The intensity of the N2, N3 and N4 components decreases with temperature: above 800 K N2 is completely suppressed, N3 reaches an almost constant value that is about a third of its initial value while N4 decreases almost linearly in the whole temperature range.

Please cite this article as: F. Orlando, et al., Synthesis of nitrogen-doped epitaxial graphene via plasma-assisted method: Role of the graphene–substrate interaction, Surf. Sci. (2015), http://dx.doi.org/10.1016/j.susc.2015.06.017

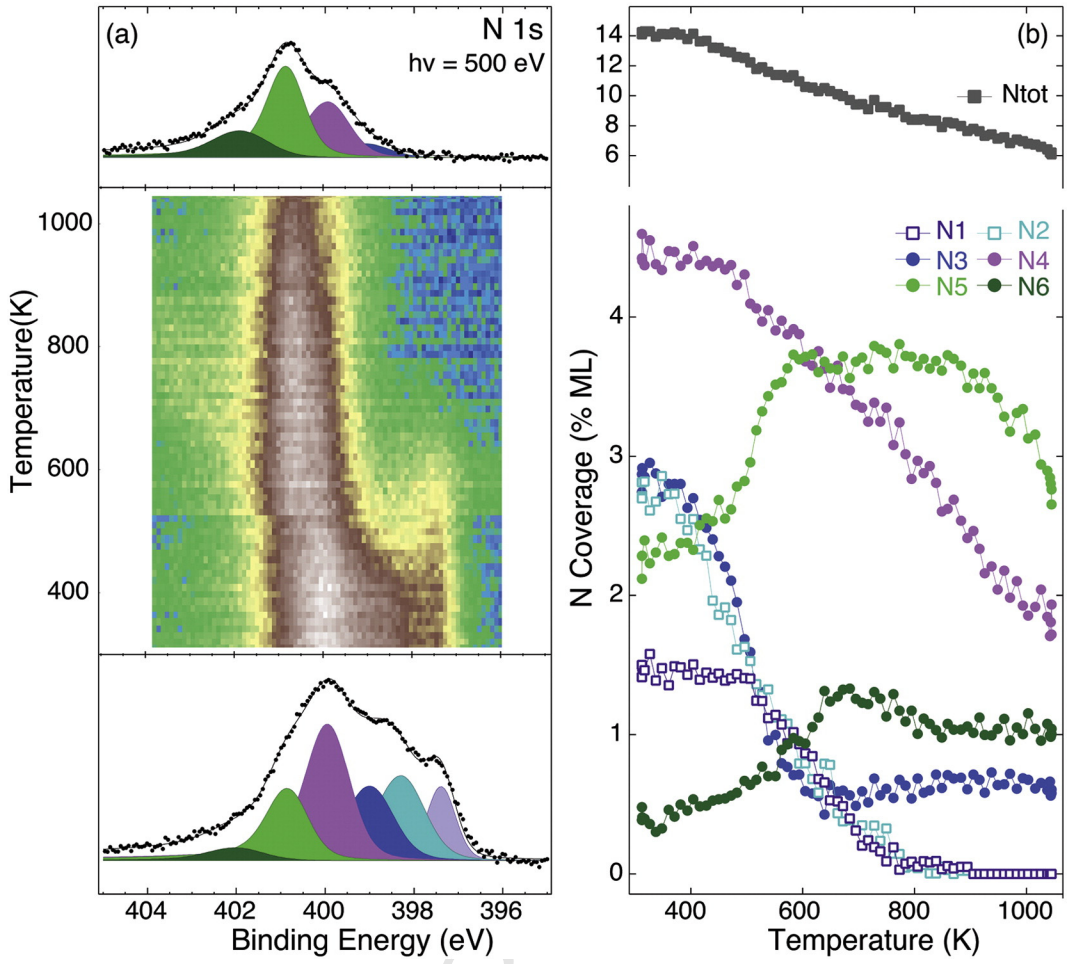

Fig. 3. (color online) (a) N 1s thermal evolution measured on GR/Ir(111) exposed to N plasma for 10 min, while ramping the temperature from 300 to 1040 K at a rate of 0.5 K/s. The bottom and top spectra were measured at room temperature before and after the annealing, respectively, while the central panel represents the N 1s intensity plot during sample heating. (b) Evolution of the N 1s total intensity (top) and of the different spectral components (bottom) during annealing, as determined from the fitting of the series of spectra of the intensity plot of the central panel in (a).

As graphitic- and pyridinic-N are expected to be the most stable species at high temperature [15,42], a large fraction of N3 has to be assigned to nitrogen atoms in pyridinic configuration. The correlation between the intensity of graphitic and pyridinic components in Fig. 3b suggests that the main conversion process is from the pyridinic to the graphitic configuration. This behavior might be interpreted in terms of a thermally activated mobility of the vacancies in the graphene network facilitating their diffusion far away from the pyridinic-N configuration, which therefore converts into graphitic-N. It has been previously reported that the N1s peak of pyridinic-N on GR/Ni(111) shifts to smaller binding energy after gold intercalation, because of the suppressed substrate interaction of pyridinic-N [25]. In our case, two pyridinic species can coexist as the result of a relatively strong (weak) interaction of the Ir surface at the valley (hill) regions of the GR/Ir(111) moiré structure. The conversion of pyridinic- to graphitic-N could then take place only on the hills of the moiré, where the defect diffusion is larger [43]. Given this consideration we hypothesize that N2 and N3 are associated to pyridinic nitrogen atoms in the valleys and hills of the moiré superstructure, respectively, with N3 containing a contribution also from interstitial/adatom N (see above). This is in line with the observed residual intensity of N3, i.e. the strongly interacting pyridinic component, and quenching of N2, the weakly interacting component, after sample annealing as illustrated in Fig. 3b. The interaction with the substrate can even prevent the conversion of part of the pyrrolic into substitutional N, thus justifying the high intensity of the N4 component after annealing, especially when compared to the pyridinic part. Regarding this point, however, one has also to take into account their different concentrations before the thermal treatment, with the intensity of the pyrrolic nitrogen component being almost two times larger than the pyridinic-N species (Fig. 3b).

After the annealing to 1040 K the sample contains nitrogen atoms mostly in graphitic configuration with a coverage of 0.04 ML. Further annealing to 1400 K leads to a reduction of the graphitic part to 0.014 ML (top spectrum of Fig. 1a). Remarkably, in both cases the Ir $4f_{7/2}$ spectrum (Fig. 1b, top) is almost indistinguishable from that of the pristine GR/Ir(111) (Fig. 1b, bottom). Indeed, upon annealing the IrSn component is completely depleted, while the IrS intensity is fully restored. This suggests that the interaction between the graphene layer doped mainly with graphitic-N and the Ir surface is weak and resembles that of the as-grown graphene on Ir(111). This result indicates that the graphene layer is not significantly deformed upon inclusion of substitutional nitrogen.

Fig. 4 shows the binding energy shift of the main graphene peak C1 as a function of the coverage of graphitic and pyridinic-N (N2 + N3 + N5 + N6) during the nitrogen plasma exposure (blue markers) and after annealing to high temperature (red markers) together with the N coverage behavior upon annealing shown in the inset. Upon plasma exposure the nitrogen doping of graphene induces a progressive shift of C1 towards higher binding energy up to ~100 meV. After annealing to 1040 K, when the largest fraction of the nitrogen atoms is in graphitic configuration, the shift of C1 further increases by ~200 meV. The additional annealing to 1400 K induces a

Please cite this article as: F. Orlando, et al., Synthesis of nitrogen-doped epitaxial graphene via plasma-assisted method: Role of the graphene–substrate interaction, Surf. Sci. (2015), http://dx.doi.org/10.1016/j.susc.2015.06.017

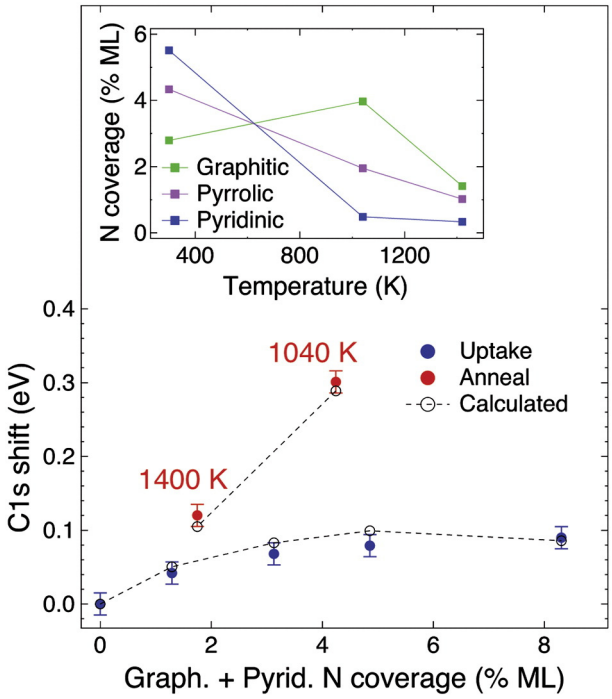

Fig. 4. (color online) Binding energy shift of the sp^2 component (C1 in Fig. 1) in the C 1s spectra as a function of graphitic and pyridinic-N coverage during exposure to N plasma and after annealing. (filled circles) experimental results; (open circles) C1s shift calculated as explained in the text. The inset shows how the coverage of pyridinic (N2 + N3), pyrrolic (N4) and graphitic-N (N5 + N6) evolve upon annealing to 1040 and 1400 K.

desorption backshift of ~180 meV. This behavior is consistent with an *n*-type doping induced by the incorporation of graphitic nitrogen in the carbon network which shifts the Dirac cone [44] as well as the core levels towards higher binding energy. In a recent investigation of GR/Ir(111) [32], we observed a shift towards lower binding energy of the C 1s peak of graphene upon oxygen intercalation, accompanied by a comparable shift of the Dirac point above the Fermi level, due to hole-doping effects caused by charge transfer from carbon to the oxygen covered Ir substrate. A similar argument can be used to interpret the shift of the main graphene peak reported in Fig. 4, the only difference being the sign of the shift due to the *n*-type doping of graphitic nitrogen. It is important to stress here that not only the nitrogen concentration but also its configuration affects the position of the Dirac point. Previous investigations on graphene as well as carbon nanotubes have shown that while graphitic nitrogen induces an *n*-type doping, the pyridinic, pyrrolic and adatom or interstitial configurations cause a *p*-type doping [25,45–47]. The largest effect is given by pyridinic nitrogen which, however, shifts the Dirac cone to lower binding energy by about a third of the energy shift of graphitic-N [25]. This explains the additional positive shift of the C 1s observed upon the first annealing to 1040 K. Indeed, this determines an increase of the graphitic-N that gives an *n*-type doping and, at the same time, a reduction of the pyridinic/pyrrolic components leading to a *p*-type doping. The subsequent annealing to 1400 K results in a large, general loss of the nitrogen atoms and, thus, the graphene peak moves back towards the undoped energy position. This picture is further confirmed by a back-of-the-envelope calculation of the C 1s shift as a function of the graphitic and pyridinic coverage illustrated by the black open circles in Fig. 4. The shift was calculated using a contribution of +80 and −25 meV/% ML of graphitic and pyridinic nitrogen, respectively, assuming that only

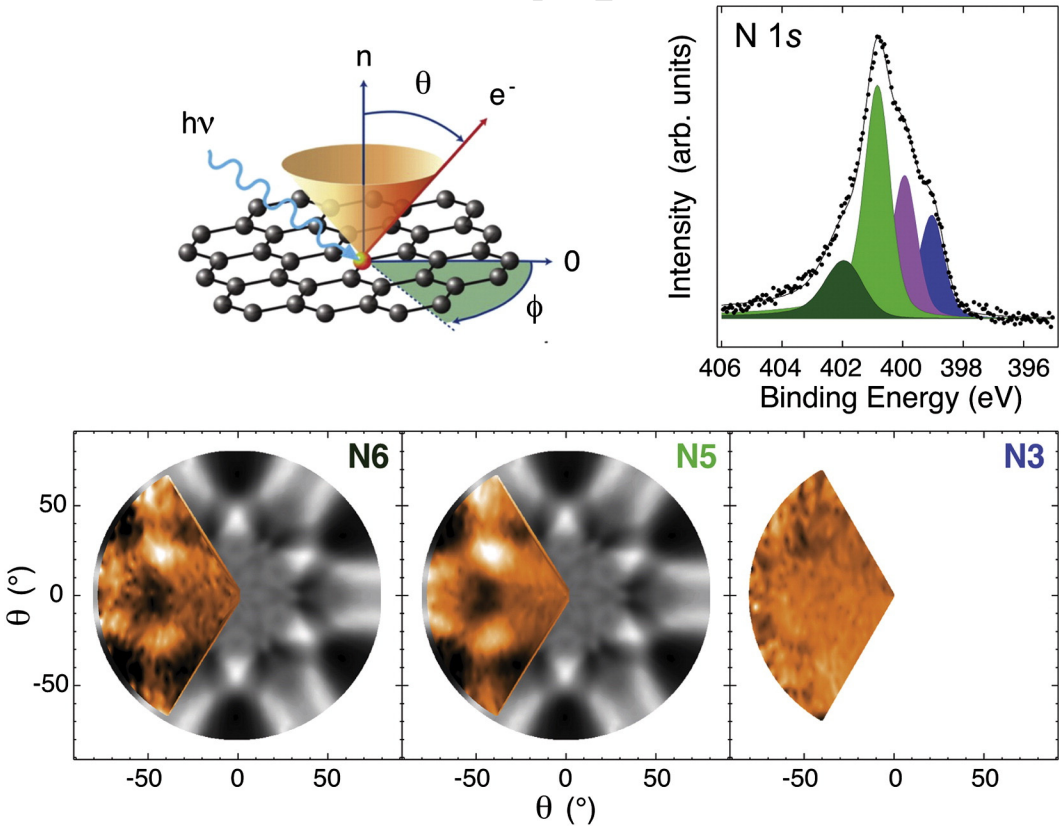

Fig. 5. (color online) Top: (left) schematic representation of the graphene lattice with the N atom in red and of the experimental geometry; (right) N1s photoemission spectrum at normal emission; bottom: stereographic projection of the integrated photoemission intensity modulation $I(\theta,\phi)$ as a function of the emission angle for the N 1s spectral components measured at $h\nu = 500$ eV, corresponding to a photoelectron kinetic energy of 100 eV (color scale) together with multiple scattering simulations calculated for a free-standing graphene layer with a graphitic nitrogen atom as emitter (gray scale). The XPD patterns of N3 and N4 are very similar and do not show any appreciable modulation. For convenience only the N3 XPD pattern is displayed on the right. (For interpretation of the references to color in this figure legend, the reader is referred to the web version of this article.)

Please cite this article as: F. Orlando, et al., Synthesis of nitrogen-doped epitaxial graphene via plasma-assisted method: Role of the graphene–substrate interaction, Surf. Sci. (2015), http://dx.doi.org/10.1016/j.susc.2015.06.017

these nitrogen species contribute to the doping of the graphene layer (then excluding the pyrrolic-N contribution, which was found to be negligible [48], that of adsorbed and interstitial N, which coverage is expected to be small, and the contribution of the nitrogen atoms adsorbed on the Ir surface). The good agreement between the experimental C 1s shift and the calculated one in the different situations further confirms the validity of this assumption. The graphitic-to-pyridinic contribution ratio to the C 1s shift of −3.2 of our work is in perfect agreement with that found in the same coverage range by Koch et al. [25], who calculated the shift of the Dirac point for the graphitic and pyridinic-N species for the GR/Au/Ni(111) system. This result indicates that the graphitic *n*-doping contribution is more than three times larger than the *p*-doping of the pyridinic species.

To gain further insight into the local environment of the N atoms, we performed XPD measurements by collecting N 1s photoemission spectra at fixed photon energy of 500 eV and different emission angles, similarly to the experiments reported in Refs. [49,50]. The measurements were carried out on a graphene layer exposed to N_2 plasma for 15 min, and subsequently annealed to 900 K in order to allow the conversion of the nitrogen species, with the maximum concentration of graphitic-N (see Fig. 3). However, it should be noted that in the present case the relative coverage of the N3 component due to pyridinic-N (Fig. 5) is higher than that of the sample discussed so far. This is most probably due to the more prolonged N plasma dose (15 min instead of 10 min) which allows the formation of more pyridinic-N, as can be extrapolated from Fig. 1d. The presence of all these components allowed us to get insight into the structure of graphitic, pyrrolic and pyridinic-N species. The bottom part of Fig. 5 shows the N 1s XPD patterns of the N3–N6 components. In color scale are shown the experimental results while in gray scale is displayed the multiple scattering simulation calculated for a free-standing graphene layer with a graphitic nitrogen atom as the emitter. The striking similarity between the simulation and the measured diffraction patterns of N5 and N6 further confirms the assignment of these components to nitrogen in substitutional configuration. Moreover, these results confirm that the inclusion of graphitic nitrogen does not affect the local structural geometry of the carbon network. As to pyridinic and pyrrolic-N species, the absence of any measurable modulation in their XPD pattern shows that the configuration of these species does not preserve a locally ordered structure.

4. Conclusions

In this paper we report on the functionalization of a graphene layer grown on the Ir(111) surface by nitrogen plasma treatment. Different types of bonding configurations, namely, graphitic, pyridinic and pyrrolic nitrogen were identified by means of XPS and XPD techniques. Our results indicate that the GR–Ir interaction modulates the relative concentration of these nitrogen species, as it promotes the formation of pyrrolic- and pyridinic-N. Decoupling of GR from its Ir substrate by oxygen intercalation results in the depletion of the pyrrolic and pyridinic content accompanied by the enhancement of the substitutional component. The increase of the graphitic nitrogen concentration is obtained also by annealing the sample because of the higher thermal stability of this atomic configuration and of the selective conversion of the other nitrogen species. When the substitutional nitrogen is the most abundant configuration, a weak interaction between the Ir substrate and the nitrogen-doped graphene layer is re-established, which is similar to the undoped GR/Ir(111) interface. Finally, the XPD measurements gave a direct insight on the local geometry of the graphitic nitrogen atoms embedded in the carbon network. Graphitic-N was found to lie in the graphene plane while pyridinic and pyrrolic-N species do not show any modulation due to the lack of local order. The possibility to vary the concentration of nitrogen species by thermal annealing and by tuning the GR-substrate interaction is of importance for tailoring the electronic properties of monolayer graphene.

Acknowledgments

We acknowledge the financial support from MIUR through the project PRIN entitled “GRAF. Frontiers in graphene research: understanding and controlling advanced functionalities” (N.20105ZZYSE001) and from the University of Trieste through the programme “Finanziamento di Ateneo per progetti di ricerca scientifica - FRA 2014”.

References

[1] F. Schwierz, Nat. Nanotechnol. 5 (2010) 487.
[2] D. Zhan, J. Yan, L. Lai, Z. Ni, L. Liu, Z. Shen, Adv. Mater. 24 (2012) 4055.
[3] W. Zhu, D. Neumayer, V. Perebeinos, P. Avouris, Nano Lett. 10 (2010) 3572.
[4] T. Ohta, A. Bostwick, T. Seyller, K. Horn, E. Rotenberg, Science 313 (2006) 951.
[5] R. Balog, B. Jorgensen, L. Nilsson, M. Andersen, E. Rienks, M. Bianchi, M. Fanetti, E. Laegsgaard, A. Baraldi, S. Lizzit, Z. Sljivancanin, F. Besenbacher, B. Hammer, T.G. Pedersen, P. Hofmann, L. Hornekaer, Nat. Mater. 9 (2010) 315.
[6] F. Schedin, A.K. Geim, S.V. Morozov, E.W. Hill, P. Blake, M.I. Katsnelson, K.S. Novoselov, Nat. Mater. 6 (2007) 652.
[7] F. Banhart, J. Kotakoski, A.V. Krasheninnikov, ACS Nano 5 (2011) 26.
[8] L. Ci, L. Song, C. Jin, D. Jariwala, D. Wu, Y. Li, A. Srivastava, Z.F. Wang, K. Storr, L. Balicas, F. Liu, P.M. Ajayan, Nat. Mater. 9 (2010) 430.
[9] Z.-H. Sheng, L. Shao, J.-J. Chen, W.-J. Bao, F.-B. Wang, X.-H. Xia, ACS Nano 5 (2011) 4350.
[10] Y. Wang, Y. Shao, D.W. Matson, J. Li, Y. Lin, ACS Nano 4 (2010) 1790.
[11] D. Wei, Y. Liu, Y. Wang, H. Zhang, L. Huang, G. Yu, Nano Lett. 9 (2009) 1752.
[12] N. Li, Z. Wang, K. Zhao, Z. Shi, Z. Gu, S. Xu, Carbon 48 (2010) 255.
[13] X. Li, W. Cai, J. An, S. Kim, J. Nah, D. Yang, R. Piner, A. Velamakanni, I. Jung, E. Tutuc, S.K. Banerjee, L. Colombo, R.S. Ruoff, Science 324 (2009) 1312.
[14] Y.-C. Lin, C.-Y. Lin, P.-W. Chiu, Appl. Phys. Lett. 96 (2010) 133110.
[15] M. Scardamaglia, B. Aleman, M. Amati, C. Ewels, P. Pochet, N. Reckinger, J.F. Colomer, T. Skaltsas, N. Tagmatarchis, R. Snyders, L. Gregoratti, C. Bittencourt, Carbon 73 (2014) 371.
[16] L. Zhao, R. He, K.T. Rim, T. Schiros, K.S. Kim, H. Zhou, C. Gutiérrez, S.P. Chockalingam, C.J. Arguello, L. Pálová, D. Nordlund, M.S. Hybertsen, D.R. Reichman, T.F. Heinz, P. Kim, A. Pinczuk, G.W. Flynn, A.N. Pasupathy, Science 333 (2011) 999.
[17] F. Joucken, Y. Tison, J. Lagoute, J. Dumont, D. Cabosart, B. Zheng, V. Repain, C. Chacon, Y. Girard, A.R. Botello-Méndez, S. Rousset, R. Sporken, J.-C. Charlier, L. Henrard, Phys. Rev. B 85 (2012) 161408.
[18] J.C. Meyer, S. Kurasch, H.J. Park, V. Skakalova, D. Künzel, A. Groß, A. Chuvilin, G. Algara-Siller, S. Roth, T. Iwasaki, U. Starke, J.H. Smet, U. Kaiser, Nat. Mater. 10 (2011) 209.
[19] C. Zhang, L. Fu, N. Liu, M. Liu, Y. Wang, Z. Liu, Adv. Mater. 23 (2011) 1020.
[20] S. Doniach, M. Sunjic, J. Phys. C 3 (1970) 285.
[21] F.J. García de Abajo, M.A. Van Hove, C.S. Fadley, Phys. Rev. B 63 (2001) 075404.
[22] K.-J. Kim, H. Lee, J. Choi, H. Lee, M.C. Jung, H.J. Shin, T.-H. Kang, B. Kim, S. Kim, J. Phys. Condens. Matter 22 (2010) 045005.
[23] D. Usachov, O. Vilkov, A. Grüneis, D. Haberer, A. Fedorov, V.K. Adamchuk, A.B. Preobrajenski, P. Dudin, A. Barinov, M. Oehzelt, C. Laubschat, D.V. Vyalikh, Nano Lett. 11 (2011) 5401.
[24] K.-j. Kim, S. Yang, Y. Park, M. Lee, B. Kim, H. Lee, J. Phys. Chem. C 117 (2013) 2129.
[25] R.J. Koch, M. Weser, W. Zhao, F. Viñes, K. Gotterbarm, S.M. Kozlov, O. Höfert, M. Ostler, C. Papp, J. Gebhardt, H.P. Steinrück, A. Görling, T. Seyller, Phys. Rev. B 86 (2012) 075401.
[26] A. Mueller, M.G. Schwab, N. Encinas, D. Vollmer, H. Sachdev, K. Müllen, Carbon 84 (2015) 426.
[27] R. Balog, M. Andersen, B. Jørgensen, Z. Sljivancanin, B. Hammer, A. Baraldi, R. Larciprete, P. Hofmann, L. Hornekær, S. Lizzit, ACS Nano 7 (2013) 3823.
[28] P. Lacovig, M. Pozzo, D. Alfè, P. Vilmercati, A. Baraldi, S. Lizzit, Phys. Rev. Lett. 103 (2009) 166101.
[29] F. Presel, N. Jabeen, M. Pozzo, D. Curcio, L. Omiciuolo, P. Lacovig, S. Lizzit, D. Alfè, A. Baraldi, Carbon 93 (2015) 187.
[30] J.R. Pels, F. Kapteijn, J.A. Moulijn, Q. Zhu, K.M. Thomas, Carbon 33 (1995) 1641.
[31] C.J. Weststrate, J.W. Bakker, A.C. Gluhoi, W. Ludwig, B.E. Nieuwenhuys, Catal. Today 154 (2010) 46.
[32] R. Larciprete, S. Ulstrup, P. Lacovig, M. Dalmiglio, M. Bianchi, F. Mazzola, L. Hornekær, F. Orlando, A. Baraldi, P. Hofmann, S. Lizzit, ACS Nano 6 (2012) 9551.
[33] A. Barinov, O.B. Malcioğlu, S. Fabris, T. Sun, L. Gregoratti, M. Dalmiglio, M. Kiskinova, J. Phys. Chem. C 113 (2009) 9009.
[34] L.H. Chan, K.H. Hong, D.Q. Xiao, T.C. Lin, S.H. Lai, W.J. Hsieh, H.C. Shih, Phys. Rev. B 70 (2004) 125408.
[35] M. Bianchi, D. Cassese, A. Cavallin, R. Comin, F. Orlando, L. Postregna, E. Golfetto, S. Lizzit, A. Baraldi, New J. Phys. 11 (2009) 063002.
[36] R. Larciprete, S. Fabris, T. Sun, P. Lacovig, A. Baraldi, S. Lizzit, J. Am. Chem. Soc. 133 (2011) 17315.
[37] A. Cavallin, M. Pozzo, C. Africh, A. Baraldi, E. Vesselli, C. Dri, G. Comelli, R. Larciprete, P. Lacovig, S. Lizzit, D. Alfè, ACS Nano 6 (2012) 3034.
[38] C. Vo-Van, S. Schumacher, J. Coraux, V. Sessi, O. Fruchart, N.B. Brookes, P. Ohresser, T. Michely, Appl. Phys. Lett. 99 (2011) 142504.
[39] S. Lizzit, R. Larciprete, P. Lacovig, K.L. Kostov, D. Menzel, ACS Nano 7 (2013) 4359.
[40] A. Baraldi, G. Comelli, S. Lizzit, D. Cocco, G. Paolucci, R. Rosei, Surf. Sci. 367 (1996) L67.

Please cite this article as: F. Orlando, et al., Synthesis of nitrogen-doped epitaxial graphene via plasma-assisted method: Role of the graphene–substrate interaction, Surf. Sci. (2015), http://dx.doi.org/10.1016/j.susc.2015.06.017

[41] A. Kumar, A. Ganguly, P. Papakonstantinou, J. Phys. Condens. Matter 24 (2012) 235503.
[42] F. Xu, M. Minniti, P. Barone, A. Sindona, A. Bonanno, A. Oliva, Carbon 46 (2008) 1489.
[43] E. Miniussi, M. Pozzo, A. Baraldi, E. Vesselli, R.R. Zhan, G. Comelli, T.O. Menteş, M.A. Niño, A. Locatelli, S. Lizzit, D. Alfè, Phys. Rev. Lett. 106 (2011) 216101.
[44] A. Lherbier, X. Blase, Y.-M. Niquet, F. Triozon, S. Roche, Phys. Rev. Lett. 101 (2008) 036808.
[45] M. Zhao, Y. Xia, J.P. Lewis, R. Zhang, J. Appl. Phys. 94 (2003) 2398.
[46] S.H. Lim, R. Li, W. Ji, J. Lin, Phys. Rev. B 76 (2007) 195406.
[47] S. Jalili, R. Vaziri, Mol. Phys. 109 (2011) 687.
[48] B. Wang, L. Tsetseris, S.T. Pantelides, J. Mater. Chem. A 1 (2013) 14927.
[49] F. Orlando, P. Lacovig, L. Omiciuolo, N.G. Apostol, R. Larciprete, A. Baraldi, S. Lizzit, ACS Nano 8 (2014) 12063.
[50] S. Lizzit, G. Zampieri, L. Petaccia, R. Larciprete, P. Lacovig, E.D.L. Rienks, G. Bihlmayer, A. Baraldi, P. Hofmann, Nat. Phys. 6 (2010) 345.

Please cite this article as: F. Orlando, et al., Synthesis of nitrogen-doped epitaxial graphene via plasma-assisted method: Role of the graphene–substrate interaction, Surf. Sci. (2015), http://dx.doi.org/10.1016/j.susc.2015.06.017